The International Journal of Advanced Manufacturing Technology (2020) 107:205–216
https://doi.org/10.1007/s00170-020-05089-0

ORIGINAL ARTICLE

Effect of structural parameters of array of holes in the tube electrode for electrochemical cutting

Tao Yang [1] · Yongbin Zeng [1] · Yumeng Sang [1] · Shouye Li [1]

Received: 7 August 2019 / Accepted: 9 February 2020 / Published online: 14 February 2020
© Springer-Verlag London Ltd., part of Springer Nature 2020

Abstract
Wire electrochemical machining is a highly flexible machining method based on the electrochemical dissolution of a workpiece anode, which corrodes. Material is removed locally from the workpiece as the tool is moved through two dimensions. In electrochemical cutting using a tube electrode, a metal tube with an array of holes on the sidewall replaces the conventional wire as the tool cathode. The electrolyte enters through the top of the tube electrode, is ejected though the array of holes, and directly sprays onto the machining surface of the workpiece. In this paper, the flow of the electrolyte in the machining gap was simulated for tube electrodes with different holes spacing and inclination angles. Experiments verified that the refreshment of the electrolyte and the removal of electrolysis products were fast and the machining efficiency was high when the holes spacing was 1 mm and inclination angle was −45°. Adding supplementary electrolyte into the slit improves the consistency of the slit width. Finally, using the optimized structural parameters, arrays of columns were fabricated from 10-mm-thick stainless steel 304 at a feed rate of 7 μm/s.

Keywords Electrochemical cutting · Tube electrode with array holes · Holes spacing · Inclination angle

1 Introduction

Electrochemical machining (ECM) is a processing technology based on the electrochemical anodic dissolution of a metal in an electrolyte. This corrodes and removes material locally from the anode workpiece. There is no tool wear during processing, no residual machining stress, and no recast layer on the machined surface. Moreover, the machining efficiency is high [1]. It has been applied for manufacturing aero-engine turbine disk, blade, integral blisks, diffuser, propeller hub, and other precision parts [2]. Wire electrochemical machining (WECM) uses a metal wire as the tool cathode, which is feed in two dimensions relative to the anode workpiece during cutting [3]. It is a highly flexible form of machining.

In anodic dissolution, reduction reactions occur on the tool surface forming bubbles of hydrogen, while oxidation reactions occur on the workpiece surface to create insoluble electrolysis products. In addition, joule heat is produced by currents passing between the tool cathode, electrolyte, and anode workpiece [4]. For WECM, due to the narrow and deep gap between the wire electrode and the workpiece, it is difficult to remove the hydrogen bubbles and insoluble products, which changes the composition and concentration of the electrolyte, reduces the electrolytic reaction rate and machining accuracy, and seriously hinders the machining [5].

To accelerate the flow of electrolyte and promote the removal of electrolysis products, many improvements have been applied. An acidic electrolyte can used to dissolve the insoluble electrolysis products, which is conducive to their removal [6]. At present, this method is used only in micro-ECM because some of the acid will be consumed during processing, which changes the composition of the electrolyte after a long time. Moreover, the acidic waste electrolyte is difficult to recycle and treat, so this method is not friendly to the environment [7]. Another WECM technique is to add additional movements to one of the electrodes. For example, a reciprocating movement of the wire electrode (which has a dragging effect on the electrolyte in the machining gap) [8], anode vibration (which has a throwaway effect on the electrolyte in the machining gap) [9], and high-speed rotation of the cylindrical electrode (which

✉ Yongbin Zeng
binyz@nuaa.edu.cn

[1] Jiangsu Key Laboratory of Precision and Micro-Manufacturing Technology, Nanjing University of Aeronautics and Astronautics, Nanjing 210016, China

creates a disturbance in the electrolyte in the machining gap) [10]. These approaches can promote the flow of electrolyte and accelerate the movement of electrolysis products. In WECM with axial electrolyte flushing, a high-speed flow of electrolyte along the wire electrode axis into the machining gap washes out the electrolysis products [11]. In electrochemical cutting using a tube electrode and normal electrolyte flushing [12], the tool cathode is a metal tube with a closed end and an array of holes on the sidewall. The electrolyte flushes out the electrolysis products and fresh electrolyte sprays from the array of holes into the machining gap.

To enhance the mass transmission in the machining gap, further accelerate the electrolytic reactions, and improve the machining efficiency, the structure of the cathode can be optimized. For WECM with a reciprocating movement of the wire electrode, Xu et al. [13] used chemical etching to corrode the surface of the electrode slightly. This increased the surface roughness of the wire electrode and enhanced its ability to carry electrolysis products. He et al. [14] fabricated microstructures on the surface of a smooth wire electrode using micro-laser direct scanning machining, and compared the machining efficiency and accuracy with those of a smooth wire electrode. The experimental results show that the machining efficiency was improved by 1.5 times for the wire electrode with a surface microstructure. Zou et al. [15] fabricated microgrooves on the surface of rod electrodes using micro-WECM, which made the electrodes ribbed. Through comparative experiments, they proved that the machining efficiency of WECM had doubled. For anode-vibration-aided WECM, Meng et al. [16] successfully used a tool cathode made of helical carbon nanotube fibers to machine metallic glass made of an amorphous material. For WECM in which the cylindrical electrode is rotated at high speed, Fang et al. [17] experimentally compared a helical electrode and a rod electrode on WECM machining efficiency. The experimental results for an electrode of stainless steel 304 with a rotary cutting edge as the tool cathode for WECM [18] show that the machining efficiency was improved by 1.5 times compared to a cylindrical wire electrode. For WECM with axial electrolyte flushing, Klocke et al. [19, 20] used two twisted metal wires as tool cathodes in electrochemical cutting experiments on direct-aged Inconel 718 with a thickness of 40 mm. The cutting rate was up to 20 mm^2/min.

For electrochemical cutting using a tube electrode with an array of holes, the important structural parameters of the cathode are the spacing and the inclination angle of the array holes, which affect the electrolyte flow velocity and flow rate, the current density in the machining gap, and thus, the machining efficiency and accuracy. However, the effect of these structural parameters on electrochemical cutting has not been reported, and this is the focus of this paper. The effect of the spacing and inclination angle of the holes on the electrolyte flow velocity and flow rate in the machining gap were studied by simulation, whereas the effect on machining result was verified experimentally. In addition, adding a nozzle to provide supplementary electrolyte to the slit was adopted to reduce the difference in the widths of the upper and lower parts of the slit and thus, to improve the consistency of the slit width. Finally, using the optimized structural parameters, a square array of columns and a fan-shaped array of columns were fabricated from 10-mm-thick stainless steel 304 at a feed rate of 7 μm/s.

2 Machining process and experimental details

Fig. 1(a) is a schematic of electrochemical cutting using a tube electrode. The tube electrode is a closed stainless steel tube at the bottom. During processing, the high-pressure electrolyte enters the inner cavity through the upper end of the tube electrode, and then sprays out from the array holes on the sidewall. High-speed flow of electrolyte directly reaches the machining area to participate in electrolytic reaction, which can improve the efficiency of electrochemical cutting. Meanwhile, electrolysis products are quickly washed out of the machining area, which can speed up the removal of electrolysis products. In addition, the workpiece moves upward and downward in the process of feed movement [12]. Fig. 1(b) shows various tube electrodes with holes at different inclination angles. The spacing is the distance between two adjacent holes in the array. The inclination angle is the angle at which the holes axis is inclined from the horizontal.

The experimental setup is shown in Fig. 2. The main parts are a machine tool with *X*-, *Y*-, and *Z*- axes, an electrolyte circulation system, a high-frequency short-pulse power supply, a digital oscilloscope, a tube electrode, and a cathode

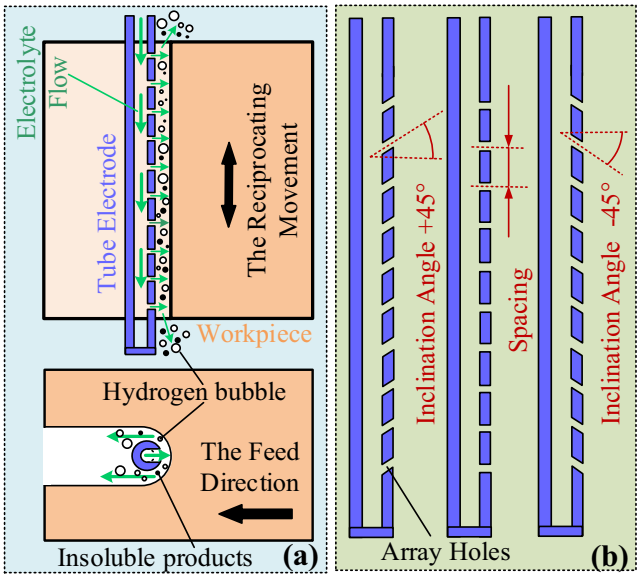

Fig. 1 Schematic of electrochemical cutting using a tube electrode. (a) Machining. (b) Tube electrodes with holes at different inclination angles

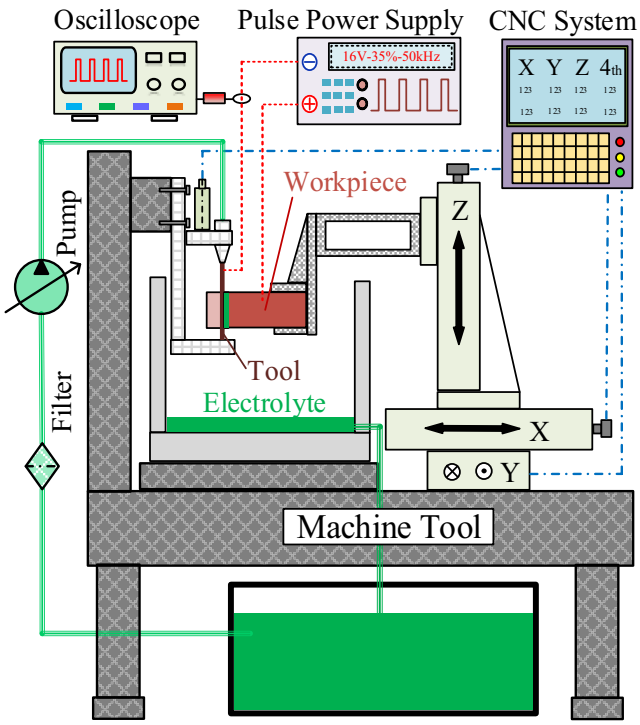

Fig. 2 Schematic diagram of the experimental setup

clamp. The cathode clamp, which is fixed on the machine tool, holds the tube electrode in place. The workpiece is fed along the *XY* plane, while the reciprocating movement of the workpiece is driven along the *Z*-axis. The circulation of the electrolyte is driven by a pump. It is filtered before entering the pump. The high-frequency short-pulse power supply provides the electric energy needed for the electrolytic reactions. It is important in achieving the efficiency and accuracy of ECM.

The workpiece (stainless steel 304) was polished and ultrasonically cleaned before the experiment. The tool cathode is a commercial stainless steel tube with an outside diameter of 0.3 mm and an inside diameter of 0.15 mm. One end was closed by micro-laser welding and the array of holes was machined by micro-laser drilling. The spacing and number of array holes were set at 0.5 mm and 20, 1.0 mm and 10, 1.5 mm and 7, and 2.0 mm and 5, respectively. The reciprocating amplitude was equal to the spacing of the holes to ensure that the electrolyte spray covered the entire machining surface. In this case, the change of reciprocating frequency has a very weak effect on the machining result. This is because that the electrolyte is always sprayed in the machining gap during the reciprocating movement of the workpiece. The reciprocating frequency changes the flow of electrolyte in the local region of the machining gap, but has a very weak effect on the overall flow velocity of the electrolyte in the machining gap and the flushing effect of the electrolyte on the electrolysis products. This explanation has been verified in the study of reference [12]. Moreover, the experiment result of this reference [12] also indicated that the machining results are best when the reciprocating frequency is 1.5 Hz. Therefore, in order to explore the effect of the spacing of array holes on the machining results, the reciprocating frequency of the workpiece was fixed at 1.5 Hz in this study. The experimental parameters were as listed in Table 1.

In WECM, the machining efficiency is determined by the maximum feed rate (MFR), which is the highest achievable feed rate with no short circuits. Moreover, the machining accuracy is determined from the average slit width, the slit width standard deviation, and the surface roughness of slit wall. At the end of a test run, the slit width and the slit wall surface roughness were measured using an microscope (SMT7-SFA, Olympus) and a form and surface measurement (FTS-5, Taylor), respectively. The average slit width s and the standard deviation of the slit width σ are defined as

$$s = \frac{1}{n}\sum_{i=1}^{n} b_i \tag{1}$$

and

$$\sigma = \sqrt{\frac{\sum_{i=1}^{n}(b_i - s)^2}{n-1}} \tag{2}$$

where b_i are the measured widths of the machined slit and n = 10in this study.

3 Simulation analysis

3.1 Simulation model

Fig. 3 shows the simulation model of electrolyte flow field in the whole machining area. Table 2 lists the calculation parameters.

In this study, the continuity equation and Navier-Stokes equation are adopted, and the standard $\kappa - \varepsilon$ model is chosen as the turbulence model of the flow field simulation. In order to simplify the flow field simulation and improve the efficiency of simulation, bubbles and insoluble products were not

Table 1 Experimental parameters

Parameter	Value
Diameter of holes (mm)	0.15
Spacing of holes (mm)	0.5, 1.0, 1.5, 2.0
Inclination angle (°)	+45, 0, −45
Workpiece	SS304, thickness 10 mm
Electrolyte	$NaNO_3$, 10 wt%
Inlet pressure (MPa)	2.0
Electrical parameters	16 V, 50 kHz, 35%
Reciprocating amplitude (mm)	Spacing of holes

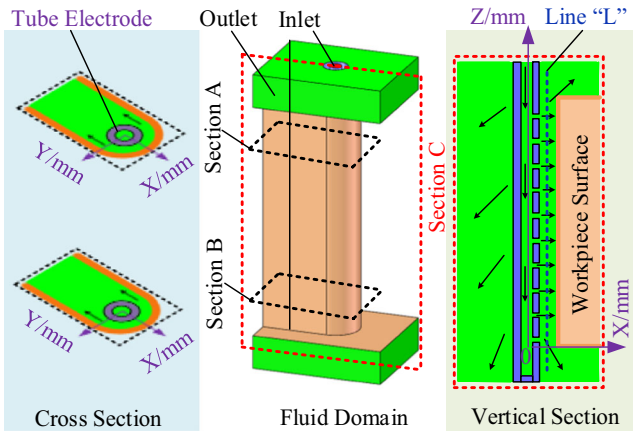

Fig. 3 Flow field model in the whole machining area

considered in the simulation calculation. Because the electrolyte in the machining gap is ejected through the array holes on the tube electrode, and the flow velocity is very fast. The bubbles and insoluble products in the machining gap are flushed out by the flow energy of the electrolyte, and the removal rate mainly depends on the flow velocity of the electrolyte. Moreover, the flow field analysis in this study was mainly to explore the effect of the spacing and inclination angle of array holes on the flow state of electrolyte in the machining gap. The simulation using a single liquid phase can reflect the flow velocity distribution of electrolyte in machining gap. The flow state of the electrolyte in the whole machining area was simulated by ANSYS Fluent 17.0.

3.2 Effect of array holes spacing

Fig. 4 Shows the flow velocity contours of the electrolyte at cross section C (the cross section C is the plane Y = 0 mm) for different holes spacing. Figs. 5 and 6 present, respectively, the electrolyte flow velocity at line L (the line L is the line X = 0.2 mm and Y = 0 mm) and the flow rate in the machining gap for different holes spacing. The entire machining gap was always filled with electrolyte, which flowed quickly through the gap. When the inlet pressure was constant, the average flow velocity of the electrolyte at line L increases, but the flow rate of the electrolyte in the whole machining are gradually decreased with the increase of holes spacing

When the spacing of array holes is large, the holes number of electrolyte flowing from the tube electrode to the machining gap reduce, compared with that of the array holes spacing is small. The pressure of electrolyte in the tube electrode is large, and the velocity of injection into the machining gap is high. Therefore, the average flow velocity of the electrolyte at line L increases with the increase of holes spacing. However, with a small spacing of array holes, the holes number of electrolyte flowing from the tube electrode to the machining gap increase, compared with that of the array holes spacing is large. Therefore, when the spacing of array holes decreases, the flow rate of electrolyte in the machining gap increases.

Table 2 Simulation parameters

Parameter	Value
Outside diameter of tool cathode (mm)	0.3
Inside diameter of tool cathode (mm)	0.15
Diameter of holes (mm)	0.15
Spacing of holes (mm)	0.5, 1.0, 1.5, 2.0
Inclination angle (°)	+45, 0, −45
Workpiece thickness (mm)	10
Slit width (mm)	0.5
Cutting slit length (mm)	0.75
Electrolyte inlet pressure (MPa)	2.0

3.3 Effect of array holes inclination angles

The effect of the inclination angles of the holes is discussed. The spacing and number of holes were 1.0 mm and 10, respectively. The inclination angles was +45°, 0°, or − 45°. The simulation parameters are shown in Table 2. The flow velocity contours of the electrolyte are given in Fig. 7. The entire machining gap was always filled with electrolyte, and the electrolyte flowed quickly through the gap. However, the flow velocity of the electrolyte depends on the inclination angle. When the inclination angle was +45°, the electrolyte flow velocity in region A was higher than in region B. That is, the flow velocity of the electrolyte in the upper part of the machining gap was higher than in the lower part. When the inclination angle was 0°, the electrolyte flow velocity in region A was not significantly different from that in region B. When the inclination angle was −45°, the electrolyte flow velocity was lower in region A than in region B. That is, the flow velocity of the electrolyte in the upper part of the machining gap was lower than in the lower part.

Changing the inclination angle changes the direction in which the electrolyte is sprayed onto the workpiece machining surface, as shown in Fig. 8. When the inclination angle was +45°, the electrolyte sprayed onto the workpiece machining surface with an upward inclination of 45°, then bounced back in the machining gap. The electrolyte flowed upward in the machining gap. When the inclination angle was −45°, the electrolyte sprayed onto the workpiece machining surface with a downward inclination of 45°, then bounced back in the machining gap. The electrolyte flowed downward in the machining gap. In addition, the simulation results also show that the electrolyte flow velocity in region C (Fig. 7(a)) was very high when the inclination angle was +45°. The electrolyte bounced back and upward in the machining gap, then flowed out of the machining area from the gap between the

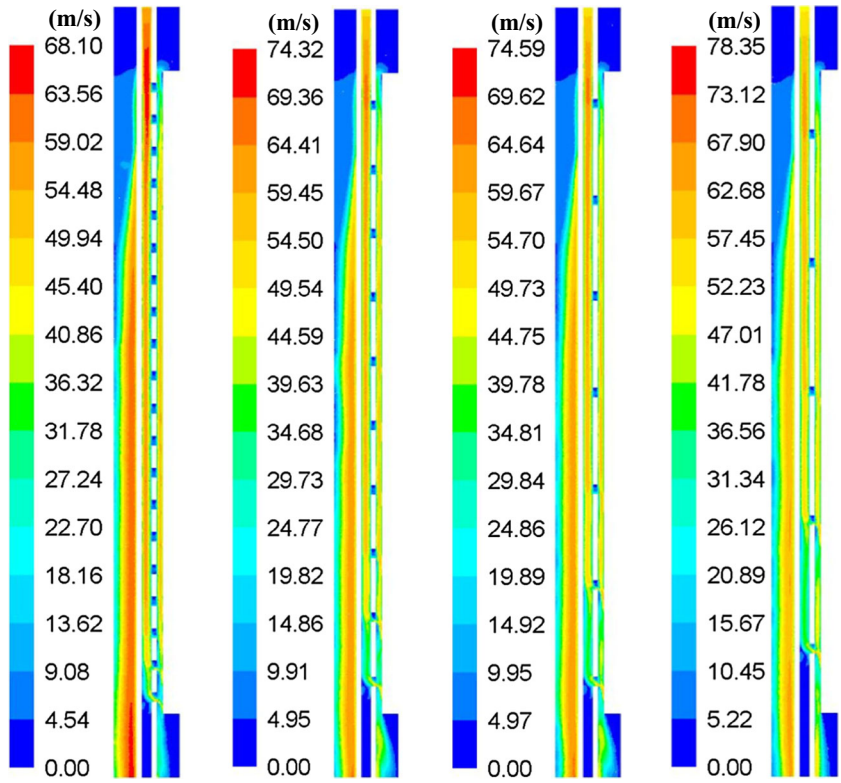

(a) Spacing = 0.5 mm (b) Spacing = 1.0 mm (c) Spacing = 1.5 mm (d) Spacing = 2.0 mm

Fig. 4 Flow velocity contours of the electrolyte at cross section C for different holes spacing

tube electrode and the machined slit, and finally, flowed out of the slit downward along the sidewall behind the tube electrode under the action of gravity.

The flow velocity at line L is shown in Fig. 9. Fig. 10 shows the average and standard deviation of the flow velocity. When the inclination angle was +45°, the average flow velocity was lowest, and highest when the inclination angle was −45°. The standard deviation of the average flow velocity was approximately the same in all cases. When the inclination angle was 0°, the electrolyte sprayed horizontally onto the workpiece machining surface. When the inclination angle was +45°, the flow velocity of the electrolyte can be divided into a horizontal component v_0 and an upward vertical component v_1. When the inclination angle was −45°, the flow

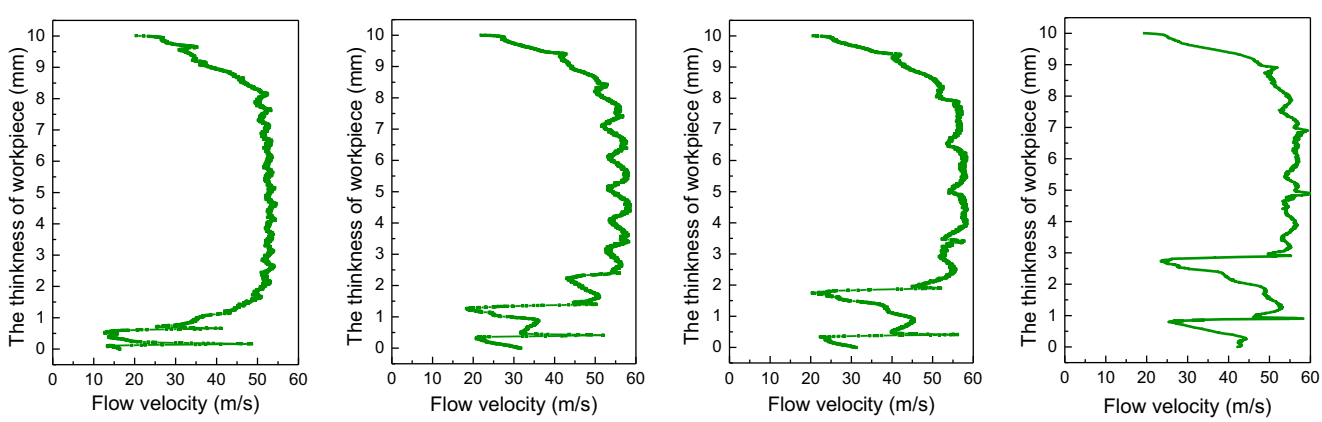

(a) Spacing = 0.5 mm (b) Spacing = 1.0 mm (c) Spacing = 1.5 mm (d) Spacing = 2.0 mm

Fig. 5 Distribution curve of flow velocity of electrolyte at line L for different holes spacing

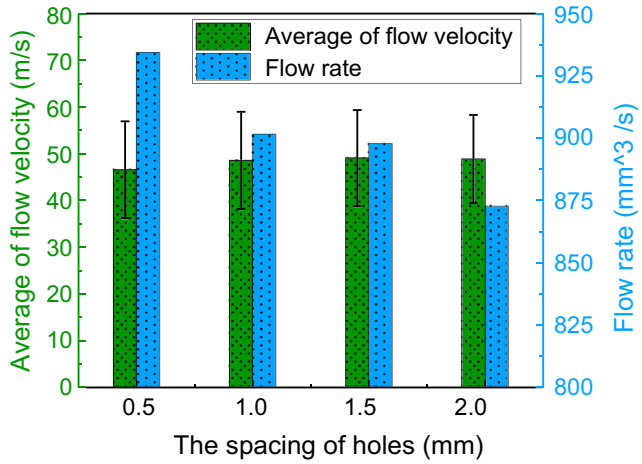

Fig. 6 Average flow velocity of electrolyte at line L and flow rate of the electrolyte in the whole machining gap for different holes spacing

velocity of the electrolyte can be divided into a horizontal component v_0 and a downward vertical component v_2. v_2 is greater than v_1 because of gravity, so the average of the flow velocity is relatively high when the inclination angle was −45°.

4 Results and discussion

4.1 Effect of array holes spacing

Fig. 11 shows the initial state for different holes spacing. The MFRs, the slit widths and surface roughness at the MFR are shown in Fig. 12. When the spacing between the holes increased from 0.5 mm to 1.0 mm, the MFR clearly increased.

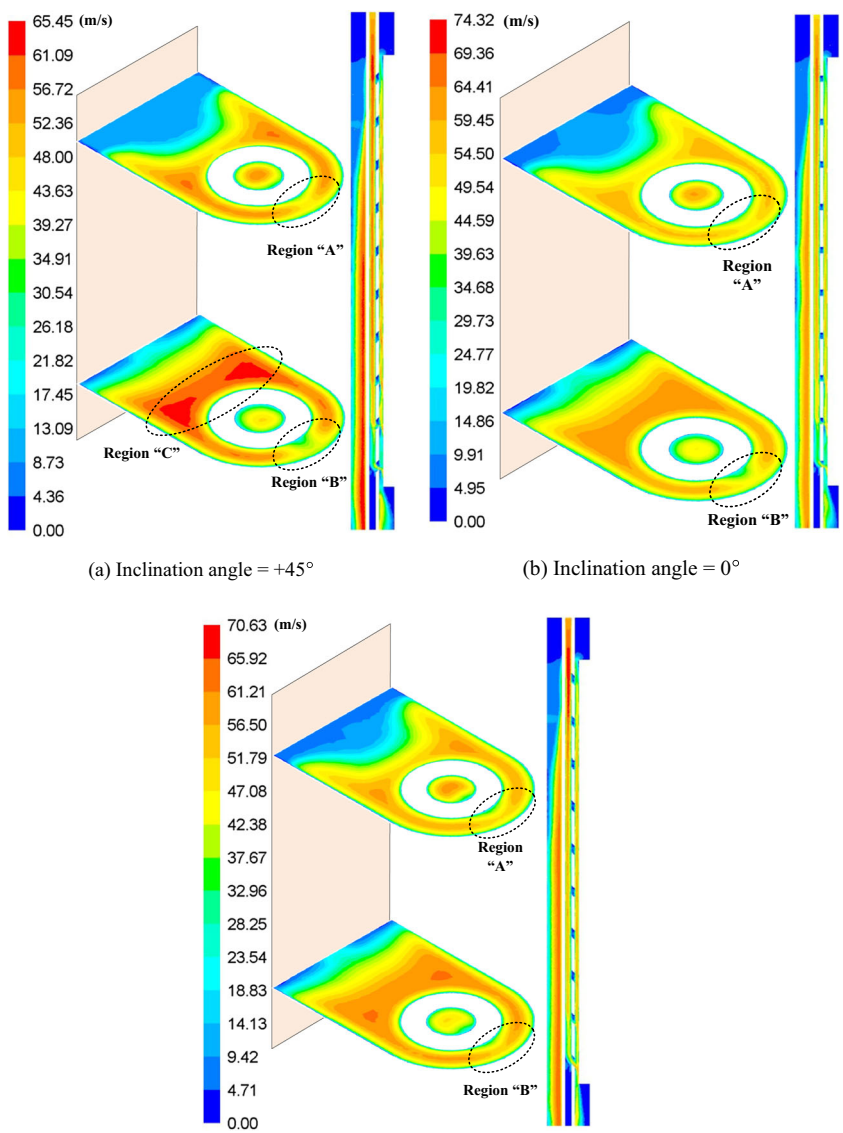

(a) Inclination angle = +45°

(b) Inclination angle = 0°

(c) Inclination angle = -45°

Fig. 7 Flow velocity contours of the electrolyte for different inclination angles

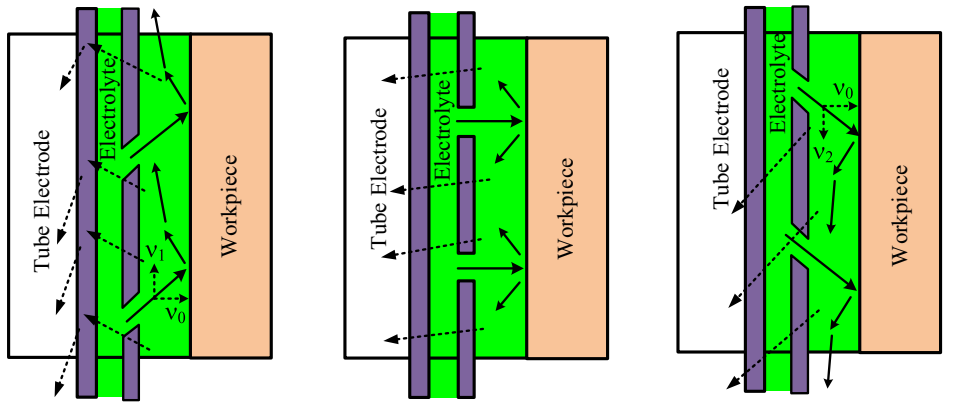

(a) Inclination angle = +45° (b) Inclination angle = 0° (c) Inclination angle = -45°

Fig. 8 Schematic of electrolyte flow in the machining gap for different inclination angles

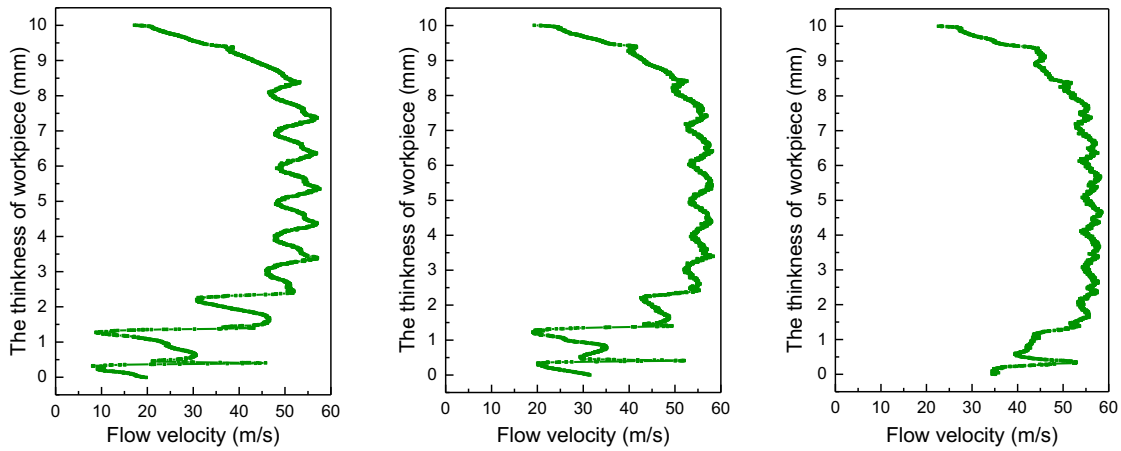

(a) Inclination angle = +45° (b) Inclination angle = 0° (c) Inclination angle = -45°

Fig. 9 Distribution of flow velocity of electrolyte at line L for different inclination angles

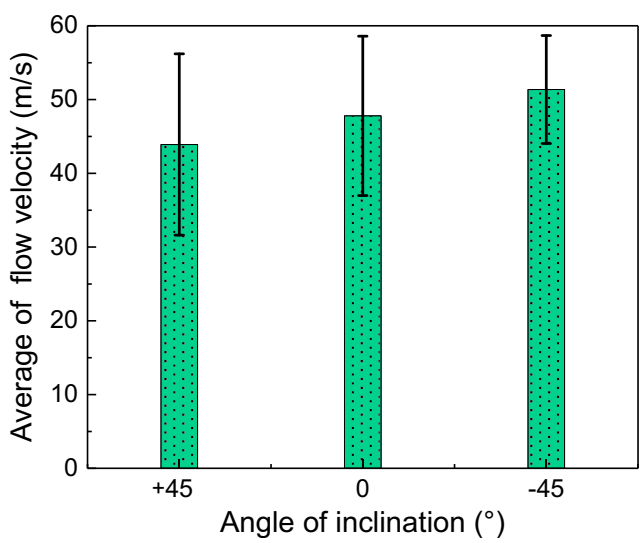

Fig. 10 Average and standard deviation of the flow velocity of electrolyte at line L for different inclination angles

As the spacing of array holes increases, the conductive area of tube electrode and the current density in the machining gap increase. The greater the current density of the machining area is, the faster the material removal rate, so the MFR increases. However, when the spacing between the holes was increased above 1.0 mm, the MFR decreased. This is because there were fewer holes and the electrolyte flow rate was lower with the increase of the holes spacing. The relative volume ratio of electrolysis products increased and the conductivity of the electrolyte decreased when the electrolyte flow rate in the whole machining are decreased (according to Eq. (3)). Therefore, the MFR decreased because of the low conductivity (according to Eq. (4)).

The conductivity of the electrolyte [21] is

$$\kappa = \kappa_0 \frac{2(1-\beta)}{2+\beta} \tag{3}$$

where κ_0 is the initial conductivity of the electrolyte and β is the fraction of electrolysis products.

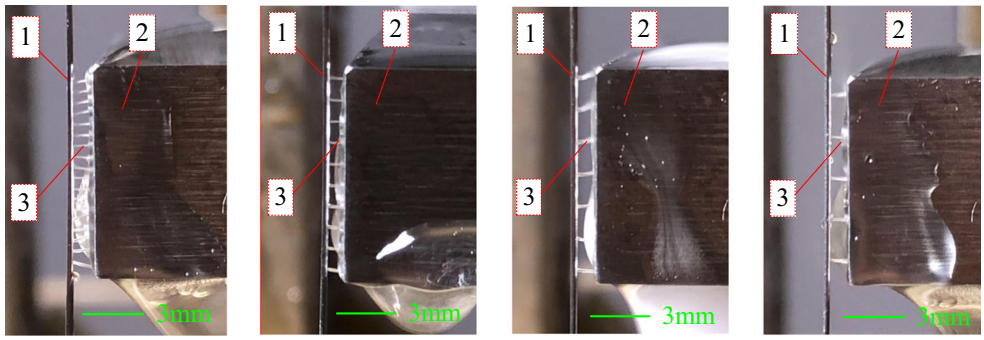

(a) Spacing = 0.5 mm (b) Spacing = 1.0 mm (c) Spacing = 1.5 mm (d) Spacing = 2.0 mm

Fig. 11 Initial state for different holes spacing (1 tube electrode, 2 anode workpiece, and 3 electrolyte)

The feed rate is given by

$$v = \eta\omega\kappa\frac{U_R}{\Delta_b} \tag{4}$$

where η is current efficiency, ω is the volumetric electrochemical equivalent, U_R is the machining voltage, and Δ_b is the inter-electrode frontal gap.

As the feed rate increases, the slit width at the MFR decreases due to the reaction time per unit length becomes shorter and the material removal amount decreases. Eqs. (4), (5) and (6) [21] also reveals the relationship between slit width and feed rate. Therefore, when the spacing of the holes increased from 0.5 mm to 1.0 mm, the slit width decreased due to the increase of the MFR. When the spacing of the holes ≥1.0 mm, with an increase of the hole spacing, the slit width at the MFR gradually increased due to the decrease of the MFR.

$$\Delta_s \cong \Delta_b\sqrt{1+\frac{2D_T}{\Delta_b}} \tag{5}$$

$$D_s = D_T + 2\Delta_s \tag{6}$$

where Δ_s is the side machining gap, D_T is the diameter of the tube electrode, and D_s is the width of machined slit.

The surface roughness of the slit wall decreases with the increase of array hole spacing. As the spacing of array holes increases, the conductive area of tube electrode and the current density in the machining gap increase. The greater the current

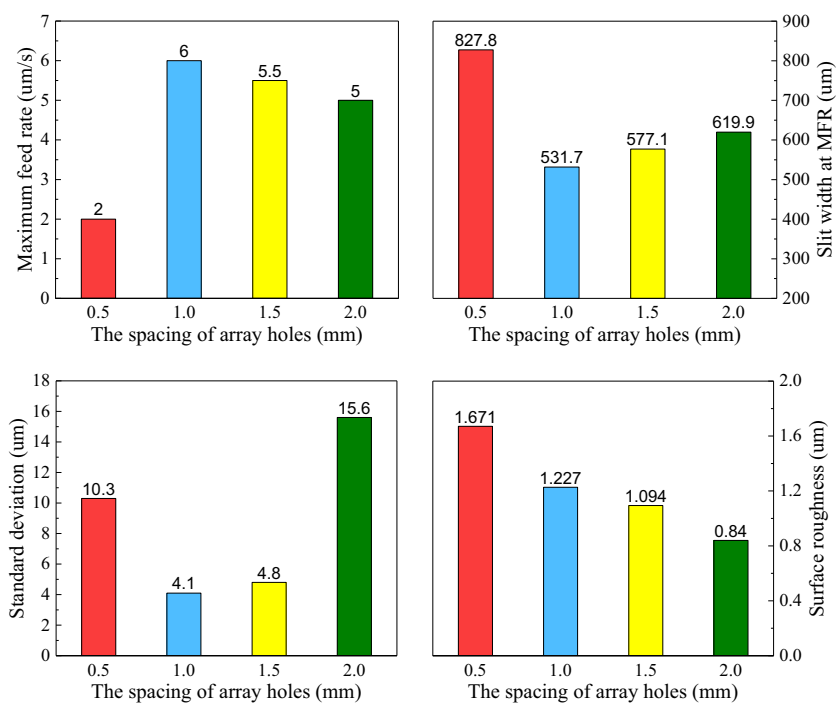

Fig. 12 The machining result for different holes spacing

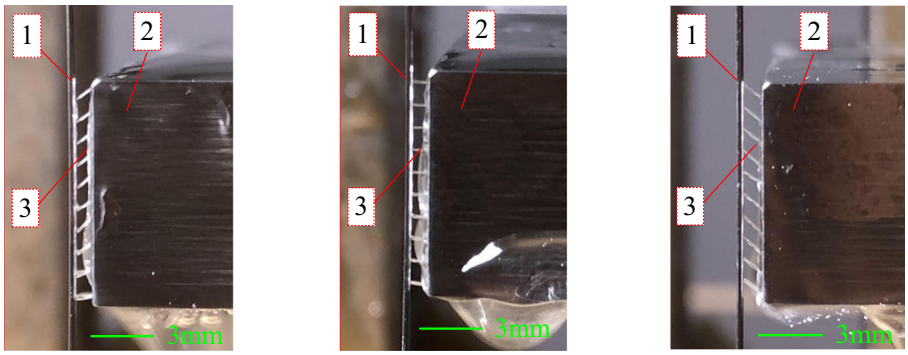

(a) Inclination angle = +45° (b) Inclination angle = 0° (c) Inclination angle = -45°

Fig. 13 Initial state for different inclination angles (1 tube electrode, 2 anode workpiece, and 3 electrolyte)

density of the machining area is, the smaller the roughness value of the machined surface is [22].

4.2 Effect of array holes inclination angles

The spacing and number of holes was now fixed at 1.0 mm and 10, respectively. Next, the effect of the inclination angle of the holes on machining is discussed. The inclination angles was +45°, 0°, or − 45°. Fig. 13 shows the initial state for different inclination angles. The effect of array holes inclination angles on the machining result is shown in Fig. 14. With the change of array holes inclination angles, the surface roughness of the slit wall is very similar, but the MFR and slit width at MFR change. When the inclination angle is 0°, the MFR is relatively low and the slit width at the MFR is relatively narrow. This is because the electrolyte sprayed horizontally onto the workpiece machining surface and then bounced back in the machining gap, and finally, flowing out of the machining area from the gap between the tube electrode and the machined slit. The total amount of electrolyte used for electrolytic reactions in the machining area was relatively small due to the rapid outflow of the electrolyte from the machining area. Moreover, the vertical component of the flow velocity was small, and the refreshment of the electrolyte in the region between two adjacent holes was slower than near a hole although the workpiece moves up and down. According to Eqs. (3) and (4), if the removal of electrolysis products is slow, the volume ratio of electrolysis products is high, and the conductivity of the electrolyte is low, then the MFR will be low.

When the inclination angle was +45° or − 45°, the MFR was relatively high and the slit width at the MFR was relatively large. This is because the electrolyte was sprayed obliquely

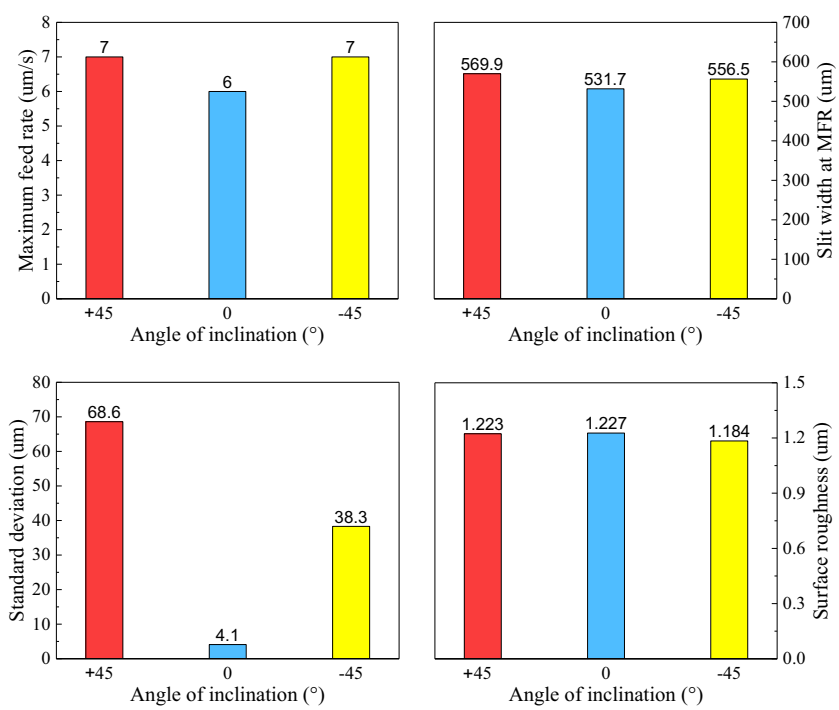

Fig. 14 The effect of inclination angles on machining result

onto the workpiece machining surface. The horizontal velocity of the electrolyte affected the electrolysis products near the workpiece machining surface, which accelerated their removal. The vertical component of the velocity of the electrolyte accelerated the flow of the electrolyte and promoted the refreshment of the electrolyte. According to Eqs. (3) and (4), if the removal of electrolysis products is fast, the volume ratio of electrolysis products is low, and the conductivity of the electrolyte is high, then the MFR will be high. In addition, the slit width at the MFR is relatively larger because of the more material removal amount, compared with that when the inclination angle is 0°.

Fig. 15 shows photographs of the side of the machined slit for different inclination angles. Combined with Fig. 14, it can be seen that the standard deviation of the slit width is significantly higher for −45° and + 45° than for 0° because of the difference between the slit widths in the upper and lower parts of the slit. For an inclination angle of +45°, the electrolyte ejected from the array of holes flows upward. Moreover, the workpiece reciprocating movement promotes the electrolyte flow in the vertical direction. The electrolyte in the machining gap flows from the bottom to the top, so that the electrolyte in the upper part flows more and faster, while the electrolyte in the lower part flow less and slower. Therefore, the machined slit is wide at the upper part and narrow at the lower part. In contrast, when the inclination angle is −45°, the machined slit is narrow at the upper part and wide at the lower part.

In addition, the standard deviation of the slit width is larger when the inclination angle is +45° than when the inclination angle is −45°. This is because of the longer path taken by the electrolyte, as explained above (Fig. 8). For an inclination angle of +45°, the flow travel time and the retention time of the electrolyte are both longer, which leads to more secondary ECM. Moreover, there are more electrolytic products in the electrolyte in the lower part, and the difference in the electrolyte conductivity between the upper and lower parts of the slit is larger. Therefore, the difference in the slit width between the upper and lower parts of the slit is greater, and so is the standard deviation of the slit width.

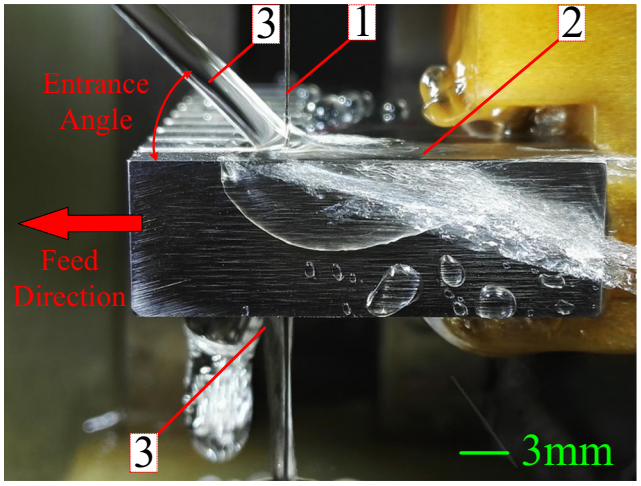

Fig. 16 Machining with additional electrolyte. (1 tube electrode, 2 anode workpiece, and 3 electrolyte)

4.3 Machining with supplementary electrolyte

Since the widths of the upper and lower parts of the slit produced by electrochemical cutting using a tube electrode with inclined holes are different, a nozzle to provide a large amount of supplementary electrolyte to the slit was adopted to reduce the difference in slit widths. A large amount of electrolyte is injected into the slit, which can reduce the difference in the amount of electrolyte between the upper and lower parts of the slit. Moreover, the increased amount of electrolyte can also wash out more of the waste electrolyte and take away more of the joule heat produced by processing in the slit.

For this experiment, a tube electrode with an inclination angle of −45° was selected. The nozzle diameter was 2.4 mm. The electrolyte flow rate and the entrance angle are 55 L/h and 45° respectively. The other machining parameters were unchanged. Fig. 16 is a photograph of machining with this configuration. Fig. 17 shows the width of the slit produced under different machining conditions. The difference between the upper and lower parts of the slit was reduced and the consistency of slit width was improved by supplying

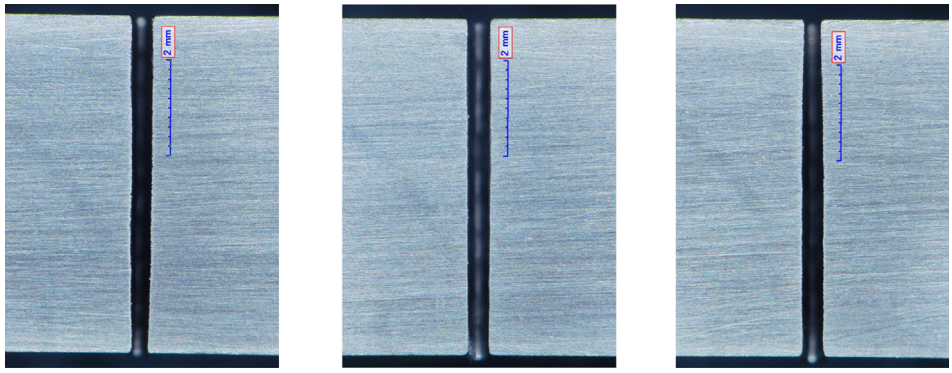

(a) Inclination angle = +45° (b) Inclination angle = 0° (c) Inclination angle = -45°

Fig. 15 Photographs of the side of the machined slit for different inclination angles

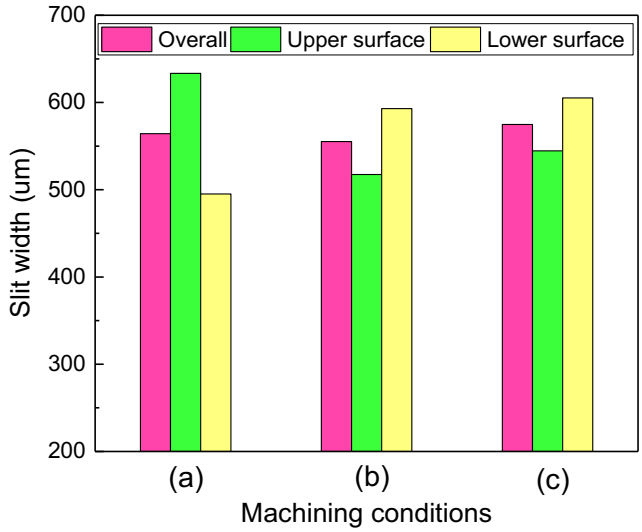

Fig. 17 Slit width under different machining conditions. (a) With an inclination angle of +45°

additional electrolyte into the slit. However, the average slit width increased slightly due to secondary ECM caused by the large amount of electrolyte in the slit.

4.4 Fabrication of an array of columns

From the above work, the structural parameters of the array of holes in the tube cathode were as follows: 10 holes 1.0 mm apart inclined at −45°. The amplitude and frequency of workpiece reciprocating movement were 1.0 mm and 1.5 Hz, respectively. Under the condition of no supplementary electrolyte, a square array of columns with a spacing of 551 μm (standard deviation of 34.36 μm) was successfully fabricated in 10-mm-thick stainless steel 304 at a feed rate of 7 μm/s, as shown in Fig. 18. This demonstrates the machining capability of electrochemical cutting using tube electrode with array holes of inclination angle is −45°. Under the condition of supplementary electrolyte, a fan-shaped array of columns with a spacing of 562 μm (standard deviation of 19.48 μm) was successfully fabricated on a stainless steel rod with a diameter of 10 mm at a feed rate of 7 μm/s, as shown in Fig. 19. This demonstrates that the method of supplementary electrolyte can reduce the standard deviation of the slit width without reducing the machining efficiency.

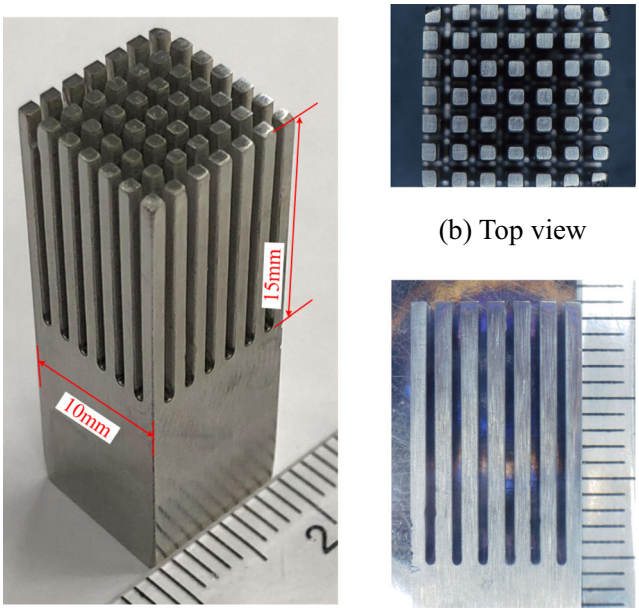

(a) 3D view (b) Top view (c) Front view

Fig. 18 Square array of columns machined using a tube electrode with an inclination angle of −45° and no supplementary electrolyte

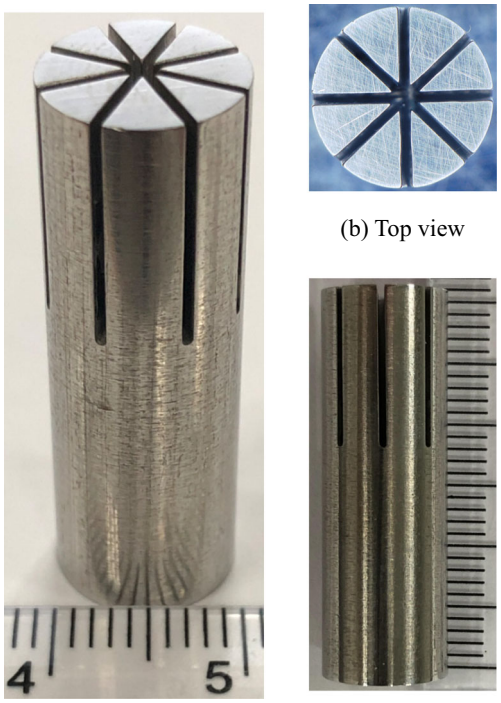

(a) 3D view (b) Top view (c) Front view

Fig. 19 Fan-shaped array of columns machined using a tube electrode with an inclination angle of −45° and supplementary electrolyte

5 Conclusions

In electrochemical cutting using tube electrode with an array of holes, the effect of the structural parameters of the array holes on machining result was investigated. The machining efficiency could be improved by using optimized structural parameters for the array holes. Our conclusions can be summarized as follows:

(1). The spacing and number of the holes in the tube electrode affect the flow rate of the electrolyte and current

density in the machining gap, and thus the machining efficiency, and accuracy. The machining efficiency of electrochemical cutting using a tube electrode with holes spacing of 1.0 mm is 3 times that with holes spacing of 0.5 mm.

(2). The inclination angle of array holes has a significant effect on the flow state of electrolyte in the machining gap. The refreshment of electrolyte and the removal of electrolysis products are fast and the machining efficiency is high when the holes inclination angle was −45°.

(3). The difference in the slit width between the upper and lower parts of the slit can be reduced and the consistency of slit width can be improved by supplying additional electrolyte to the slit. By comparing the machining results of the two arrays structure, it can be seen that the standard deviation of the slit width can be reduced from 34.36 μm to 19.48 μm with supplementary electrolyte.

(4). Using optimized machining parameters, a square array of columns and a fan-shaped array of columns were fabricated from 10-mm-thick stainless steel 304 at a feed rate of 7 μm/s.

(5). Further optimizing the diameter of the array holes and machining parameters to improve the machining efficiency and accuracy of electrochemical cutting using tube electrode.

Funding information This project was supported by the National Natural Science Foundation of China (51975291), the Natural Science Foundation of Jiangsu Province (BK20192007), and the Postgraduate Research & Practice Innovation Program of Jiangsu Province (KYCX19_0167).

References

1. Rajurkar KP, Zhu D, McGeough JA, Kozak J, De SA (1999) New developments in electro-chemical machining. CIRP Ann - Manuf Technol 48:567–579
2. Niu S, Qu NS, Fu SX, Fang XL, Li HS (2017) Investigation of inner-jet electrochemical milling of nickel-based alloy GH4169 / Inconel 718. Int J Adv Manuf Technol 93:2123–2132
3. Sharma V, Srivastava I, Jain V, Ramkumar J (2019) Modelling of wire electrochemical micromachining (wire-ECMM) process for anode shape prediction using finite element method. Electrochim Acta 312:329–341
4. Saxena KK, Qian J, Reynaerts D (2018) A review on process capabilities of electrochemical micromachining and its hybrid variants. Int J Mach Tools Manuf 127:28–56
5. Debnath S, Kundu J, Bhattacharyya B (2017) Influence of wire electrochemical machining parameters during fabrication of micro features. Int J Precis Technol 7:103–118
6. Debnath S, Doloi B, Bhattacharyya B (2019) Review—wire electrochemical machining process: overview and recent advances. J Electrochem Soc 166:E293–E309
7. Sharma S, Jain V, Shekhar R (2002) Electrochemical Drilling of Inconel Superalloy with acidified sodium chloride electrolyte. Int J Adv Manuf Technol 19:492–500
8. Jiang K, Wu XY, Lei JG, Wu W, Li W, Diao DF (2018) Vibration-assisted wire electrochemical micromachining with a suspension of B4C particles in the electrolyte. Int J Adv Manuf Technol 97:3565–3574
9. Xu K, Zeng YB, Li P, Zhu D (2015) Study of surface roughness in wire electrochemical micro machining. J Mater Process Technol 222:103–109
10. Fang XL, Zou XH, Zhang PF, Zeng YB, Qu NS (2016) Improving machining accuracy in wire electrochemical micromachining using a rotary helical electrode. Int J Adv Manuf Technol 84:929–939
11. He HD, Qu NS, Zeng YB, Fang XL, Yao YY (2016) Machining accuracy in pulsed wire electrochemical machining of γ-TiAl alloy. Int J Adv Manuf Technol 86:2353–2359
12. Yang T, Zeng YB, Hang YS (2019) Workpiece reciprocating movement aided wire electrochemical machining using a tube electrode with an array of holes. J Mater Process Technol 271:634–644
13. Xu K, Zeng YB, Li P, Fang XL, Zhu D (2016) Effect of wire cathode surface hydrophilic when using a travelling wire in wire electrochemical micro machining. J Mater Process Technol 235: 68–74
14. He HD, Qu NS, Zeng YB, Tong PZ (2017) Improvement of hydrogen bubbles detaching from the tool surface in microwire electrochemical machining by applying surface microstructures. J Electrochem Soc 164:E248–E259
15. Zou XH, Fang XL, Chen M, Zhu D (2018) Investigation on mass transfer and dissolution localization of wire electrochemical machining using vibratory ribbed wire tools. Precis Eng 51:597–603
16. Meng LC, Zeng YB, Zhu D (2018) Helical carbon nanotube Fiber tool cathode for wire electrochemical micromachining. J Electrochem Soc 165:E665–E673
17. Fang XL, Zhang PF, Zeng YB, Qu NS, Zhu D (2016) Enhancement of performance of wire electrochemical micromachining using a rotary helical electrode. J Mater Process Technol 227:129–137
18. Zou XH, Fang XL, Zeng YB, Zhu D (2017) A high efficiency approach for wire electrochemical micromachining using cutting edge tools. Int J Adv Manuf Technol 91:3943–3952
19. Klocke F, Herrig T, Zeis M, Klink A (2018) Experimental investigations of cutting rates and surface integrity in wire electrochemical machining with rotating electrode. Procedia CIRP 68:725–730
20. Klocke F, Herrig T (2018) Klink a (2018) evaluation of wire electrochemical machining with rotating electrode for the manufacture of fir tree slots. Proc ASME Turbo Expo 6:1–6
21. Zeng YB, Yu Q, Fang XL, Xu K, Li HS, Qu NS (2015) Wire electrochemical machining with monodirectional traveling wire. Int J Adv Manuf Technol 78:1251–1257
22. Qu NS, Fang XL, Zhang YD, Zhu D (2013) Enhancement of surface roughness in electrochemical machining of Ti6Al4V by pulsating electrolyte. Int J Adv Manuf Technol 69:2703–2709

Publisher's note Springer Nature remains neutral with regard to jurisdictional claims in published maps and institutional affiliations.